Experimental investigation of the acoustic black hole for sound absorption in air

EXPERIMENTAL INVESTIGATION OF THE ACOUSTIC BLACK HOLE FOR SOUND ABSORPTION IN AIR

Abdelhalim Azbaid El Ouahabi, Victor V. Krylov and Daniel J. O'Boy

Department of Aeronautical and Automotive Engineering, Loughborough University, Loughborough, Leicestershire, LE11 3TU, UK
e-mail: V.V.Krylov@lboro.ac.uk

In the present paper, the results of the first experimental investigation of the acoustic black hole for sound absorption in air are described. To achieve the required power-law decrease in sound velocity with propagation distance the inhomogeneous acoustic waveguides earlier proposed by Mironov and Pislyakov (2002) and made of quasi-periodic ribbed structures materialising walls of variable impedance have been used. Two different samples of acoustic black holes formed by these ribbed structures have been manufactured to provide linear and quadratic decreases in acoustic wave velocity with distance. Small pieces of absorbing porous material have been inserted at the end. Measurements of the reflection coefficients for guided acoustic modes incident on the black holes have been carried out in the frequency range of 100-1000 Hz. The results show the possibility of significant reduction in the acoustic reflection without using additional absorbing materials. However, contrary to the expectations, the introduction of absorbing materials did not cause further noticeable reduction in the sound reflection coefficients.

1. Introduction

During the last decade, new physical and technical objects have been developed and investigated, called 'acoustic black holes'. The main property of acoustic black holes is that they can absorb almost 100% of the incident wave energy, which makes them attractive for applications in noise and vibration control (see e.g. [1-9]). The physical principle of acoustic black holes is based on a linear or higher order power-law-type decrease in velocity of the incident wave with propagation distance to almost zero, which should be accompanied by efficient energy absorption in the area of low velocity via small pieces of inserted absorbing materials.

So far, this effect has been investigated mainly for flexural waves in thin plates for which the required gradual reduction in wave velocity with distance can be easily achieved by changing the plate local thickness according to a power law, with the power-law exponent being equal or larger than two [10]. This principle, in combination with adding small amounts of absorbing materials, has been applied to achieve efficient damping of flexural waves in plate-like structures using both one-dimensional 'acoustic black holes' (power-law wedges with their sharp edges covered by narrow strips of absorbing materials) [1-4] and two-dimensional 'acoustic black holes' (power-law-profiled pits with small pieces of absorbing materials attached in the middle) [5, 6, 9].

There are still very few investigations of acoustic black holes for absorption of sound in gases and liquids. Such acoustic black holes could be used for sound absorption and traditional noise control [8]. The main difficulty here is to materialise a linear or higher order power-law decrease in velocity of the incident sound wave down to zero. In the first theoretical paper on acoustic black holes for sound absorption in air [11], it was proposed to use an inhomogeneous acoustic waveguide with walls of variable impedance materialised via quasi-periodic ribbed structure to achieve the required linear decrease in acoustic wave velocity with propagation distance. No inserted absorbing materials were considered in that work. A number of theoretical and experimental works considered the specially designed gradient metamaterial layers (arrays of quasi-periodic solid cylinders) to increase efficiency of acoustic absorbers in air [12-16]. However, in all these works the useful effect was achieved via using metamaterials as impedance matching devices, rather than as acoustic black holes.

In the present paper, we report the results of the first experimental investigation of the acoustic black holes for sound absorption in air. To achieve the required power-law decrease in sound velocity with propagation distance, the inhomogeneous acoustic waveguide earlier proposed by Mironov and Pislyakov [11] has been used as the basic wave retarding structure. Two different samples of acoustic black holes have been manufactured and tested.

2. Experiments

2.1 Manufacturing of the acoustic black holes

Based on the theory developed in the paper of Mironov and Pislyakov [11], two different samples of acoustic black holes formed by quasi-periodic ribbed structures materialising walls of variable impedance have been designed and manufactured to provide linear and quadratic decreases in acoustic wave velocity with distance.

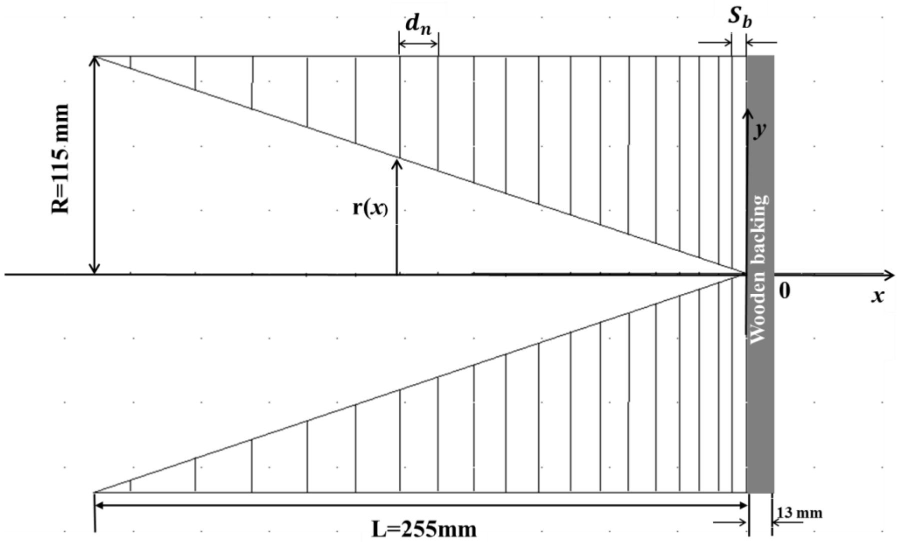

Figure 1. Schematic view of the manufactured Linear Acoustic Black Hole (LABH) showing the wooden backing and the distribution of the ribs whose inner radii decrease to almost zero.

The first structure, shown in Figure 1, has the waveguide inner radius described by a linear power law function of the distance x: $r(x) = \varepsilon_1 x^1$; it will be referred to as 'Linear Acoustic Black Hole' (LABH) in this paper. And the second structure has the inner radius as a quadratic power law function of x: $r(\mathrm{x}) = \varepsilon_2 \mathrm{x}^2$; it will be referred to as 'Quadratic Acoustic Black Hole' (QABH). Here ε_1 and ε_2 are constants. Both, LABH and QABH, consist of cylindrical plastic tubes of inner radius *R=115 mm* and length *L=255 mm* sealed at one end with a thick wooden backing of 13mm thickness. Inside the tubes, a number of solid ribs (rings) of 2 mm thickness are mounted quasi-periodically, the first rib (ring) being separated from the wooden backing by the distance $S_b = 9\,mm$ (for LABH) and by the distance $S_b = 30\,mm$ (for QABH).

The ribs (rings) have been made of laser cut steel in order to fit flush against the side of the tube wall, leaving no air gaps between the ribs' edges and the tube wall. The ribs for LABH and QABH were mounted with the increasing distances between them: $d_n = (3+n)\,mm$ and $d_n = (6+n)\,mm$ respectively, up to a maximum of 20 mm, where n is the rib number. These structures were expected to form the acoustic waveguides with varying wall admitances and varying cross sections. Inside the LABH and QABH, there were 18 ribs and 14 ribs respectively. Photographs of LABH and QABH are shown in the Figures 2(a) and 2(b) respectively.

(a)

(b)

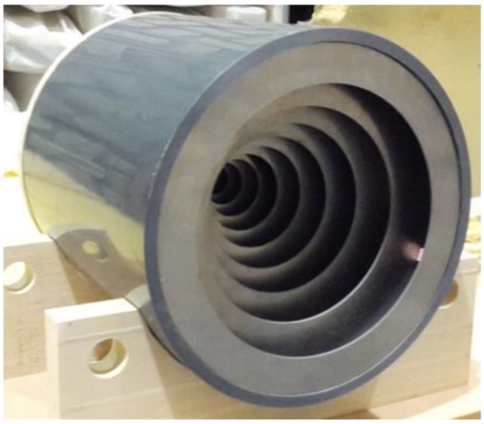

Figure 2. Photographs of LABH (a) and QABH (b)

2.2 Manufacturing of the impedance tube

Based on the two microphone transfer function method, according to the standard procedure detailed in ISO 10534-2 [17], an impedance tube made of thick plastic has been designed and manufactured with the inner diameter close to those of the samples of acoustic black holes. This was done in order to measure the reflection coefficients of incident guided modes from the black holes only, and not from the jumps in tube diameters. The interior wall was smooth enough in order to maintain low sound attenuation for the lowest order guided modes (plane waves). A hard ring has been used to hold the black hole samples with the impedance tube. On the opposite end of the tube, a loudspeaker was fixed firmly into place, and an absorbent has been placed at the loudspeaker end of the tube to reduce the effect of resonances within the impedance tube. The length of the tube has to be long enough to ensure that plane waves are fully developed before reaching the microphones and the sample, and at least half of the longest wavelength can fit in it. Therefore, the length of the tube is $L_T = 1.5\,m$, and its inner diameter is $D_T = 225\,mm$.

Fourteen holes were drilled in the tube wall for positioning the measuring microphones, separated by 50 mm between them. The first hole was separated from one end of the tube by 50 mm.

Those holes were drilled in order to enable measurements with different microphone positions and different separation between the input cross section of the sample and nearest microphone. Two holes have been used for positioning the microphones, the remaining holes have to be sealed in order to avoid air leakage into the tube. To achieve the low background noise, the tube must be sealed properly at all openings, so that the transmission loss is low.

One of the important steps in using an impedance measurement tube is knowledge of the range of frequencies for which it will yield accurate results. Plane wave can be generated in a tube only if the excitation frequency is below the cut off frequency for the 2nd acoustic mode of the tube. This frequency can be determined as [18]:

(1) $$f_u = \frac{0.58c}{D_T},$$

where c is the speed of sound, and D_T is the tube diameter. Thus, the upper limiting frequency for the tube parameters used was $f_u = 884 Hz$.

There are also restrictions on the microphone spacing [18]. In particular, the lower limiting frequency depends on the distance between the microphone positions, S_0, which should be larger than 5 % of the longest measurable wavelength. Therefore, S_0 determines the lower limiting frequency f_l using the following condition:

(2) $$f_l > \frac{0.05c}{S_0}.$$

Problems also arise, if the microphone spacing becomes too wide. This leads to an upper frequency limit due to microphone spacing given by:

(3) $$f_u < \frac{0.45c}{S_0}.$$

For the selected distance $S_0 = 150 mm$, it follows from (2) and (3) that $f_l > 114 Hz$, and $f_u < 1092 Hz$, the latter being larger than the above-determined $f_u = 884 Hz$. Consequently, the useful frequency range for the constructed impedance tube is 114 – 884 Hz.

2.3 Experimental setup

The two microphone transfer function method has been used in this work to measure the sound pressure reflection coefficients from the samples of the acoustic black holes. The experimental set-up comprised the impedance tube described above, a loudspeaker fixed at one end (it produced the constant broadband sound using the white noise generator), and two nominally identical microphones (GRAS 40E, pre-polarized ½ inch free-field). The microphones were calibrated via the same pistonphone, to measure the sound pressure. The two microphones were mounted flush with the inside wall of the tube, isolated from the tube to minimize sensitivity to vibration, and connected to a PC via a dynamic signal acquisition module NI-USB-4431 card (four analog input channels and one analog output channel) for making sound measurements. The selected spacing between the input cross section of the acoustic black holes and the nearest microphone and between the microphone positions were $L_0 = 200 mm$ and $S_0 = 150 mm$ respectively. Figure 3 shows the acoustic impedance tube with the microphones mounted on the tube. Shown are also the loudspeaker and the sample of acoustic black hole that is fixed to the end of the tube. The two microphone transfer function method was applied over a relatively large number of time samples, where the frequency response functions were processed to obtain the reflection coefficients from the two samples, LABH and QABH.

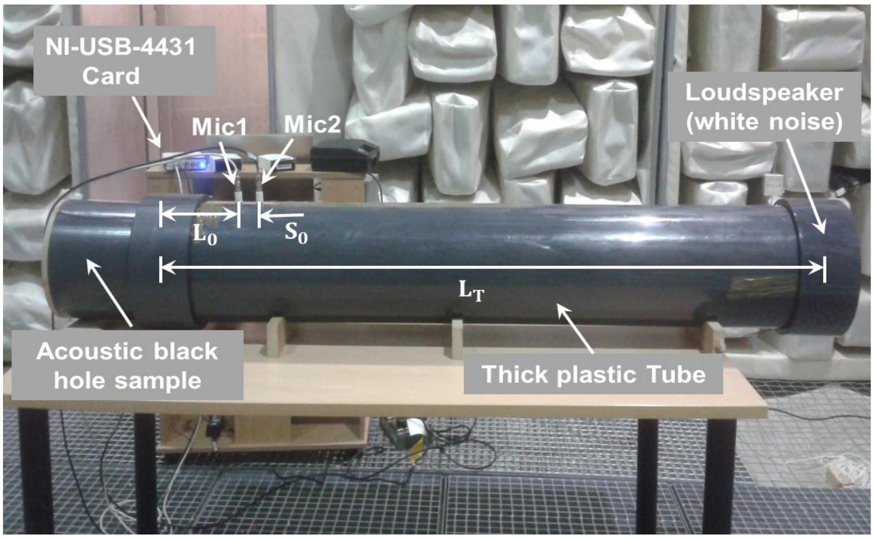

Figure 3. Photograph of the experimental set-up showing the impedance tube, two microphones mounted, a loudspeaker, the Acoustic black hole sample, and NI-USB-4431 Card: $L_T = 1.5m$, $D_T = 225mm$, $L_0 = 200mm$ and $S_0 = 150mm$.

3. Results and discussion

Measurements of the reflection coefficients from the two samples of the acoustic black holes, LABH and QABH, have been carried out in the frequency range of 100-1000 Hz. Figure 4 shows the measured sound reflection coefficients from LABH (blue line) and from QABH (red line) as functions of frequency, without using any additional absorbing materials.

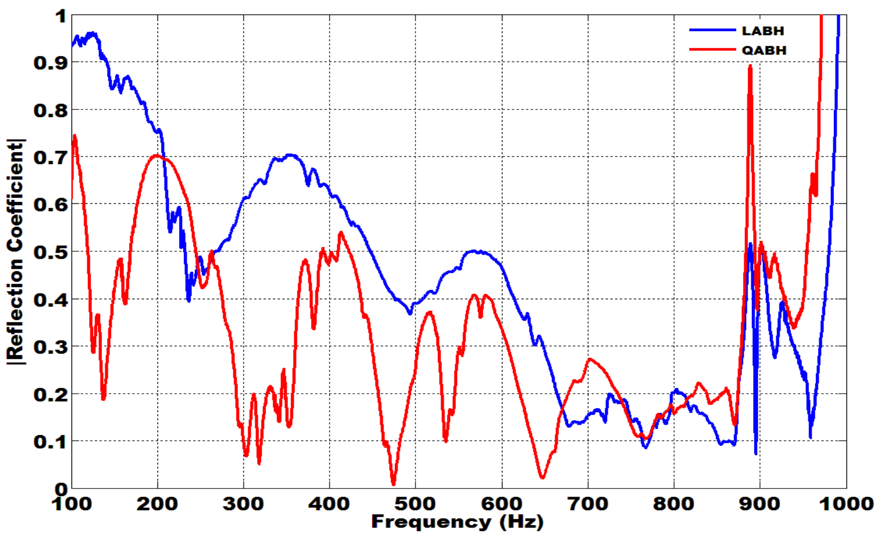

Figure 4. Frequency dependence of the sound reflection coefficients from LABH (blue line) and from QABH (red line), without using any additional absorbing materials.

The results show significant reductions in the reflection coefficients for both devices at the frequency range of 100-874 Hz. This frequency range corresponds to the useful frequency range of the constructed impedance tube. First and foremost, both curves show several maxima and minima of the reflection coefficients at that frequency range. The maximum values decrease as frequency increases for both samples, which looks similar to the theoretical prediction [11]. The value of the first maximum of the reflection coefficient for LABH is 96% at frequency 124 Hz. It drops down to about 20% at frequencies 726 Hz and 802 Hz. While the first maximum value of the reflection coefficient for QABH is 74% at frequency 104 Hz, and it decreases to 20% at frequency 860 Hz. Out of this 'useful' range of frequencies (see above) both curves exhibit various prominent sound reflection peaks, the discussion of which is beyond the scope of this paper. It can be noticed that the QABH is more efficient than LABH over the frequency range of interest.

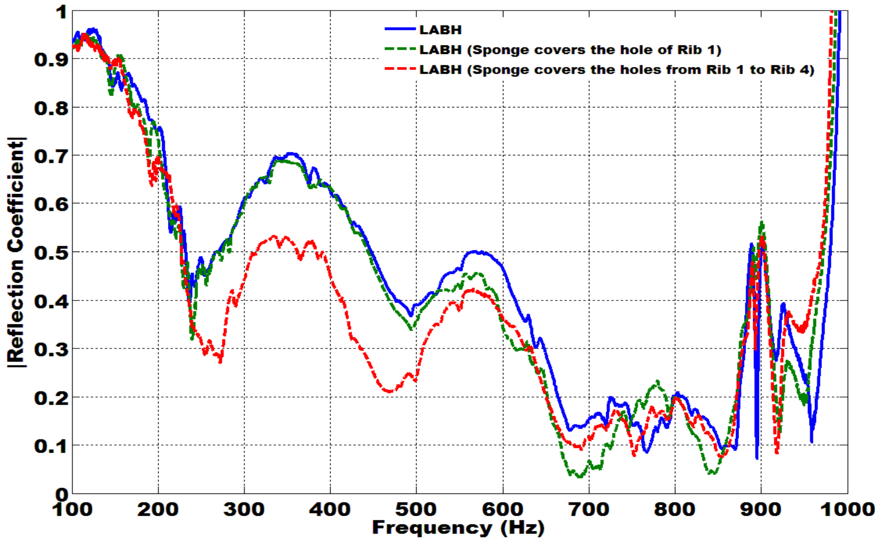

Figure 5. Frequency dependence of the sound reflection coefficients from LABH (blue line), LABH (Sponge covers the hole of Rib1) (dashed green line) and LABH (Sponge covers the holes of the first four ribs) (dashed red line).

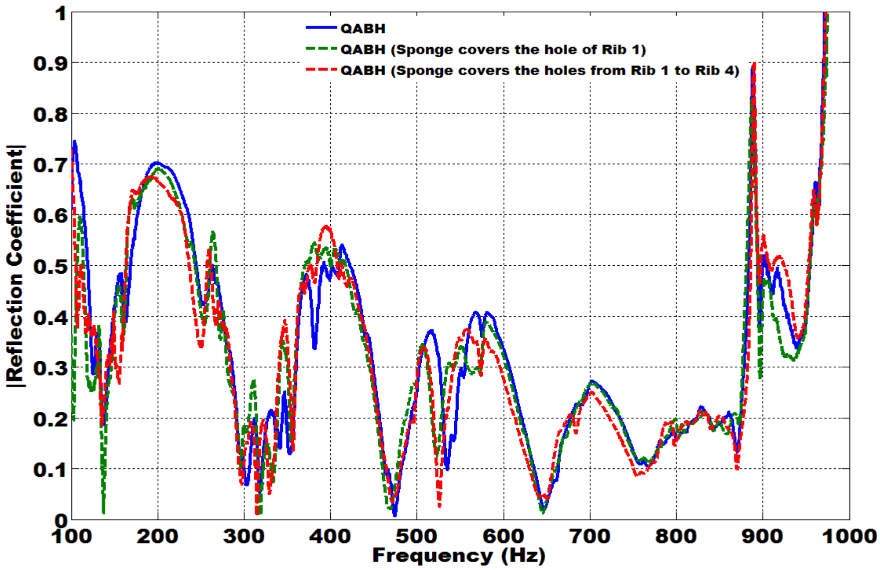

Figure 6. Frequency dependence of the sound reflection coefficients from QABH (blue line), QABH (Sponge covers the hole of Rib1) (dashed green line) and QABH (Sponge covers the holes of the first four ribs) (dashed red line).

In attempts to reduce the sound reflection coefficients from both devices even further, small pieces of absorbing porous material of conical shapes have been inserted at the end of both samples, following the ideas earlier implemented in acoustic black holes for flexural waves [1-9]. Two sizes of porous material (sponge) were used: a small one covering the first rib, and a bigger one covering the first four ribs. The results of the measurements for both LABH and QABH, without and with small pieces of sponge inserted at the end, are shown in Figures 5 and 6 respectively. It can be seen from Figure 5 that the behaviours of the reflection coefficients from LABH (with small pieces of sponge inserted at the end) and from LABH (without sponge inserted) seem to be not much different from each other, unlike in the case of acoustic black holes for flexural waves (see e.g. [1-6]). Although the LABH (with sponge covering the cavity of the first four ribs) is more efficient than the LABH (without sponge inserted), this increase in efficiency is not as large as could be expected. The measured sound reflection coefficients from QABH (with small pieces of sponge inserted at the end) and from QABH (without sponge) also do not show much difference (see Figure 6).

4. Conclusions

Two experimental samples of acoustic black holes for sound absorption in air have been manufactured and tested experimentally. It has been demonstrated that, if both experimental black holes are used without inserted porous materials, they reduce the sound reflection coefficients, and their frequency behaviour generally agrees with the theoretical predictions [11]. However, contrary to the expectations, the insertion of porous absorbing materials does not bring further significant reductions to the reflection coefficients. The reason for that is yet unclear. One of the possible explanations is that the inserted porous materials used in this work were not 'gentle' enough, so that the acoustic black hole effect was undermined by their insertion. Further experimental and theoretical investigations are required to clarify these issues and to improve the efficiency of acoustic black holes for sound absorption in air.

Acknowledgements

The research reported here has been supported by EPSRC grant EP/K038214/1. The authors would like to thank Sean Dyche for his contribution to the design of the experimental acoustic black holes and Onkar Gill for his contribution to the development of the experimental impedance tube.

REFERENCES

1 Krylov, V.V. New type of vibration dampers utilising the effect of acoustic ‘black holes’, *Acta Acustica united with Acustica*, **90**(5), 830–837, (2004).

2 Krylov, V. V. and Tilman, F. J. B. S. Acoustic ‘black holes’ for flexural waves as effective vibration dampers, *Journal of Sound and Vibration*, **274**, 605-619, (2004).

3 Krylov, V. V. and Winward, R. E. T. B. Experimental investigation of the acoustic black hole effect for flexural waves in tapered plates, *Journal of Sound and Vibration*, 300, 43-39, (2007).

4 O’Boy, D. J., Krylov, V. V. and Kralovic, V. Damping of flexural vibrations in rectangular plates using the acoustic black hole effect, *Journal of Sound and Vibration*, **329**, 4672–4688, (2010).

5 Georgiev, V. B., Cuenca, J., Gautier, F., Simon, L. and Krylov, V. V. Damping of structural vibrations in beams and elliptical plates using the acoustic black hole effect, *Journal of Sound and Vibration*, **330**, 2497–2508, (2011).

6 Bowyer, E. P., O'Boy, D. J., Krylov, V. V. and Gautier, F. Experimental investigation of damping flexural vibrations in plates containing tapered indentations of power-law profile, *Applied Acoustics*, **74**(4), 553-560, (2013).

7 Denis, V., Pelat, A., Gautier, F. and Elie, B. Modal Overlap Factor of a beam with an acoustic black hole termination, *Journal of Sound and Vibration*, **333**, 2475-2488 (2014).

8 Krylov, V.V. Acoustic black holes: Recent developments in the theory and applications, *IEEE Transactions on Ultrasonics, Ferroelectrics, and Frequency Control*, **61** (8), 1296-1306, (2014).

9 Conlon, S. C., Fahnline, J. B. and Semperlotti, F. Numerical analysis of the vibroacoustic properties of plates with embedded grids of acoustic black holes, *Journal of the Acoustical Society of America*, **137** (1), 447-457 (2015).

10 Mironov, M. A. Propagation of a flexural wave in a plate whose thickness decreases smoothly to zero in a finite interval, *Soviet Physics – Acoustics*, **34**, 318-319, (1988).

11 Mironov, M. A. and Pislyakov, V. V. One-dimensional acoustic waves in retarding structures with propagation velocity tending to zero, *Acoustical Physics*, **48** (3), 347–352, (2002).

12 Li, R., Zhu, X., Liang, B., Li, Y., Zou, X. and Cheng, J. A broadband acoustic omnidirectional absorber comprising positive index materials, *Applied Physics Letters*, **99**, 193507, (2011).

13 Climente, A., Torrent, D. and Sanchez-Dehesa, J. Omnidirectional broadband acoustic absorber based on metamaterials, *Applied Physics Letters*, **100**, 144103, (2012).

14 Umnova, O. and Zajamsek, B. Omnidirectional graded index sound absorber, *Proceedings of the Conference 'Acoustics 2012'*, Nantes, France, 23-27 April 2012, pp. 3631-3637, (2012).

15 Naify, C. J., Martin, T. P., Layman, C. N., Nicholas, M., Tangawong, A. L., Calvo, D. C. and Orris, G. J. Underwater acoustic omnidirectional absorber, *Applied Physics Letters*, **104**, 073505 (2014).

16 Azbaid El Ouahabi, A., Krylov, V. V. and O'Boy, D. J. Quasi-flat acoustic absorber enhanced by metamaterials, *Proceedings of Meetings on Acoustics* **22**, 040002, (2014).

17 ISO 10534-2, Acoustics –Determination of sound absorption coefficient and impedance in impedance tube – Part 2: Transfer-function method, (1998).

18 Cox, T. J. and D'Antonio, P., *Acoustic Absorbers and Diffusers: Theory, design and application*, 2nd Edition, Taylor & Francis, Oxford, (2009).